

# Benchmarking and quality analyses on the *All of Us* short-read structural variant catalog

Supplemental Dataset Release C2022Q4R9\_offcycle

## Introduction

Widespread benchmarking of structural variants (SVs) from short-read whole genome sequencing (srWGS) remains a significant challenge for the field of human genetics. The *All of Us* cohort of samples with srWGS SV data is unique in the availability of matched genomic datasets (i.e. single-nucleotide variant [SNV] arrays and long-read genome sequencing [lrWGS]). There also exists a number of intrinsic measures that can be used to assess the technical quality of a dataset (e.g. comparisons to external datasets, assessments of inherited variation, comparison of allele frequency spectra and variant size distributions, and population genetic principles such as Hardy-Weinberg Equilibrium). Combining these methods, we assess 7 measures of technical quality for the srWGS SV *All of Us* dataset, described in the SV Genomic Research Data Quality Report [\[1\]](#) and this supplemental document.

In the SV QC Report [\[1\]](#), we describe:

1. Variant counts (cohort-wide and per-sample) relative to gnomAD V2 [\[2\]](#) and the most recent 1000 Genomes Project high-coverage srWGS callset [\[3\]](#)
2. Size distribution of SVs
3. Hardy-Weinberg equilibrium

In this supplemental benchmarking report, we additionally describe:

4. Linkage disequilibrium with srWGS SNVs and Indels
5. Patterns of evolutionary constraint
6. Benchmarking against lrWGS
7. Benchmarking against microarrays

## Comparisons to SNVs and Indels

### Linkage disequilibrium with SNVs and Indels

### Data and Methods

Given that most common SVs segregate on haplotypes with distinct sets of SNV and small insertion and deletion variant (indel) calls, the presence of nearby SNVs and indels in linkage disequilibrium (LD) with our SV calls is an indicator of SV callset quality.

To quantify this, we computed LD between the srWGS SV joint callset and SNVs and indels from the srWGS SNP and Indel joint callset. We conducted this analysis in Hail v0.2.130 in a Python notebook backed by a Spark 3.3.0 cluster with 12 non-preemptible and 24 preemptible worker nodes. Due to the high computational resources necessary for these calculations, LD analyses were conducted on a subset of 15,001 samples. We analyzed samples from the *All of Us* genetic ancestry groups with at least 900 samples in the SV callset: European (EUR; n=46,549 samples in entire cohort), African/African American (AFR; n=24,349), Admixed American (AMR; n=15,550), East Asian (EAS; n=2,067), and South Asian (SAS; n=934). Genetic ancestry labels for each participant are based on the srWGS SNP and Indel dataset, described in the SV QC Report Appendix C [1]. We randomly selected 4,000 samples from each genetic ancestry group that contained more than 4,000 samples in the cohort (AFR, AMR, and EUR) and selected all of the samples from the EAS and SAS ancestry groups to get a total subset of 15,001 samples. We analyzed LD between all SVs with PASS filter status and SNVs and indels with PASS filter status that had a minor allele frequency of at least 1% in either the full cohort or one of these genetic ancestry groups.

LD between the callsets was computed according to the same methods used for the *All of Us* CDRv7 benchmarking and quality analyses [4]. To recap, we computed LD by first constructing two matrices:

1. An  $m \times n$  matrix  $A$  where  $m$  is the number of SV calls after minor allele frequency filtering,  $n$  is the number of samples in the cohort or genetic ancestry group, and  $A_{ij}$  is the number of alternate alleles for sample  $j$  at SV site  $i$ .
2. An  $s \times n$  matrix  $B$  where  $s$  is the number of SNVs and indels after minor allele frequency filtering and  $B_{ij}$  is the number of alternate alleles for sample  $j$  at SNV/indel site  $i$ .

We defined LD as the  $R^2$  of alternate allele dosage between each pair consisting of one SV site and one SNV site [5]. We calculated  $R^2$  values by computing the matrix multiplication  $AB^T$  after mean-centering and variance-standardizing each matrix, and then squaring each entry of the resulting correlation matrix. We limited computation to SV/SNV pairs where the SNV was within 1 megabase of the SV by defining a window extending from 1 megabase (Mb) before the start position (POS) of the SV to 1 Mb after the end position (END). Then, correlations were computed between each SV and the SNVs located within the window using Hail's block matrix sparsification functionality. For each SV we identified the SNV with which the  $R^2$  value was maximized. Given that previous LD analyses of SVs have shown that LD was much weaker for SVs that occurred in repetitive sequence contexts [2], we further subdivided the results according to the genomic context in which the SV occurs; we classified each SV as occurring in segmental duplications (SD), simple repeats (SR), other repeat-masked sequence (RM), or the unique sequence (US) outside of RM using methods from Zhao et al. 2021 [6].

## Results

A violin plot of the maximum SNV or indel  $R^2$  for each SV appears in [Figure 1](#), broken out by SV type. The median  $R^2$  of the SNV in highest LD with each SV is 0.73 for insertions, 0.14 for duplications, 0.80 for deletions, 0.88 for complex events, and 0.82 for inversions. Similar results hold when samples are subset into genetic ancestry groups ([Figure 2](#)). [Figure 3](#) shows the results of stratifying events of each SV type by the genomic sequence context it appears in. The median  $R^2$  value of the SNV in highest LD with each SV, broken into SV types within each genomic sequence context, is given in [Table 1](#). There were no inversions annotated as belonging to simple repeats in the callset. Stratifying by sequence context shows that the low overall LD of duplications was driven by events within SR or SD sequence contexts (median maximum  $R^2$  in SD: 0.14; SR: 0.05), while duplication variants within US or RM contexts have detectable LD comparable to the other SV types ([Figure 3](#); 0.83 median in US, 0.80 median in RM). It should be noted that biological factors, potentially including increased mutation rates and recombination rates in repetitive sequence contexts such as simple repeats and segmental duplications, as well as technical factors such as the difficulty of discovering SVs and SNVs in those contexts, contribute to the expected lower LD scores identified in repetitive regions of the genome. As illustrated in [Figure 4](#), in unique sequence contexts all variant classes have high median LD with a nearby SNV (INS: 0.93; DUP: 0.83; DEL: 0.93; CPX: 0.95; INV: 0.71).

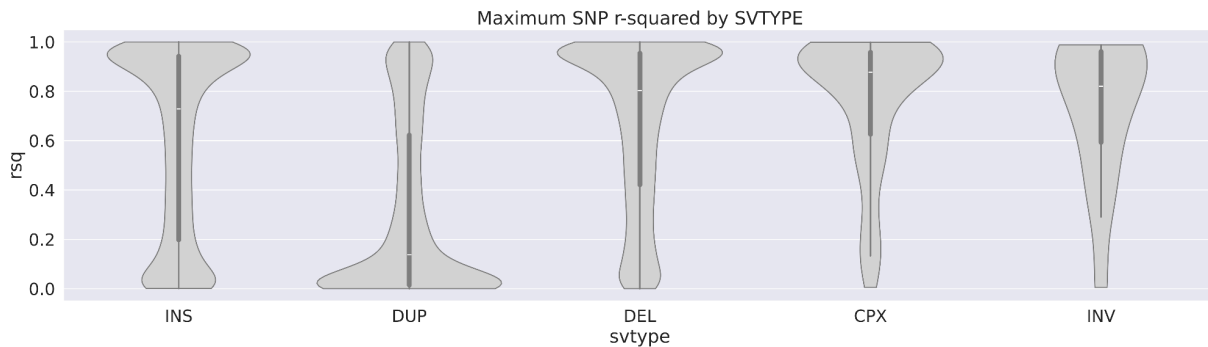


**Figure 1** – The distribution of maximum SNV-SV  $R^2$  values for each SV type. The SV types in this analysis were: deletion (DEL), duplication (DUP), insertion (INS), complex event (CPX), and inversion (INV).

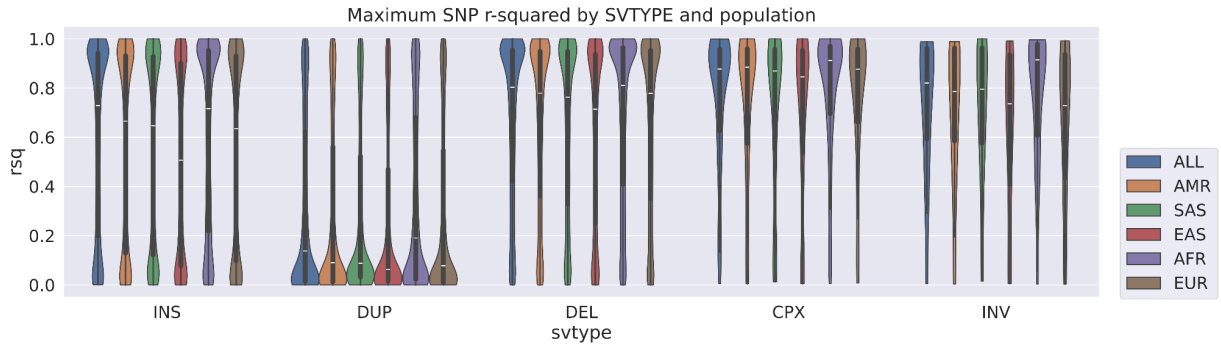


**Figure 2** – The distribution of maximum SNV-SV  $R^2$  values for each SV type, stratified by the genetic ancestry group of the participant (ALL: all samples; EAS: East Asian; AMR: Admixed American; AFR: African/African American; SAS: South Asian; EUR: European).

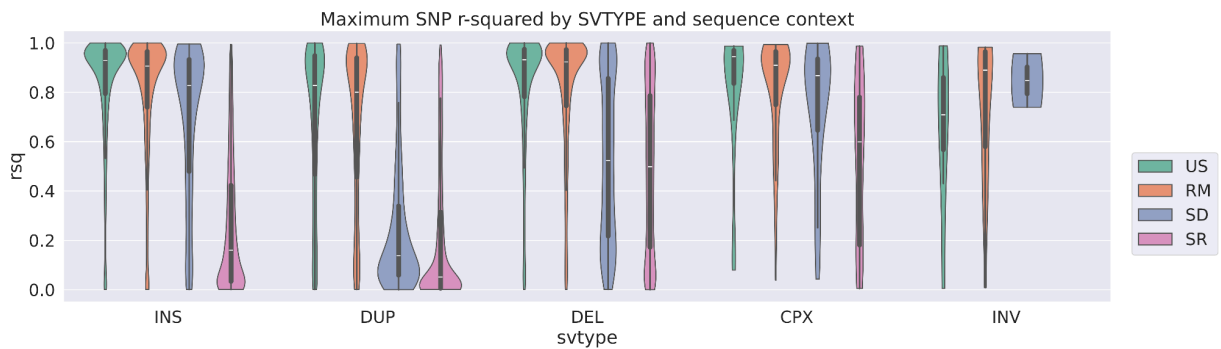


**Figure 3** – The distribution of maximum SNV-SV  $R^2$  values for each SV type, stratified by genomic context (SR: simple repeat; SD: segmental duplication; US: unique sequence; RM: repeat-masked sequence).

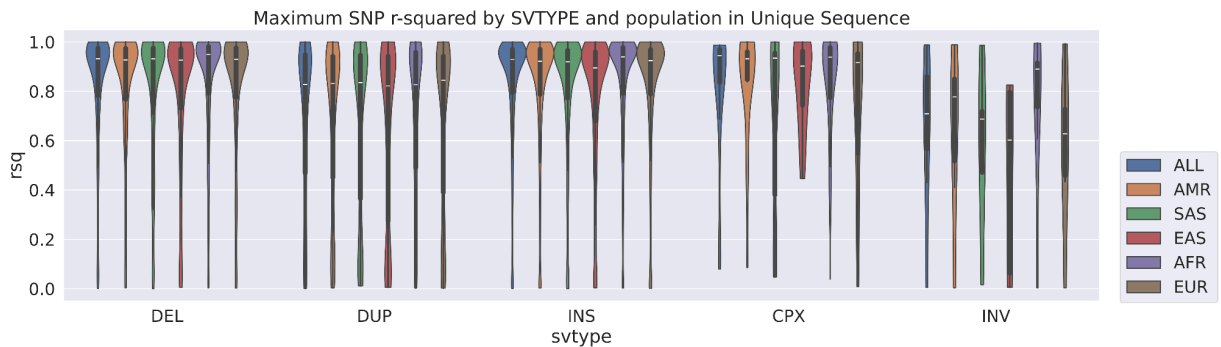


**Figure 4** – The distribution of maximum SNV-SV  $R^2$  values for each SV type when limited to regions of the genome with unique sequence context, stratified by the genetic ancestry group of the participant (ALL: all samples; EAS: East Asian; AMR: Admixed American; AFR: African/African American; SAS: South Asian; EUR: European).

**Table 1 – Median SNV-SV  $R^2$  value for each SV type, stratified by genetic ancestry groups and genomic context**

		SV Type				
Genetic ancestry group	Sequence Context	DEL	DUP	INS	CPX	INV
ALL	US	0.921	0.828	0.928	0.945	0.709
	RM	0.916	0.800	0.906	0.910	0.890
	SD	0.504	0.138	0.827	0.868	0.848
	SR	0.498	0.051	0.160	0.599	N/A
AFR	US	0.942	0.827	0.940	0.939	0.890
	RM	0.931	0.842	0.919	0.923	0.931
	SD	0.537	0.154	0.826	0.914	0.854
	SR	0.462	0.080	0.181	0.630	N/A
AMR	US	0.919	0.832	0.922	0.932	0.777
	RM	0.905	0.790	0.900	0.898	0.849
	SD	0.460	0.131	0.806	0.873	0.847
	SR	0.470	0.036	0.128	0.619	N/A
EAS	US	0.908	0.822	0.895	0.902	0.602
	RM	0.877	0.761	0.873	0.916	0.775
	SD	0.400	0.132	0.788	0.713	0.840
	SR	0.380	0.028	0.107	0.395	N/A
EUR	US	0.921	0.845	0.924	0.916	0.628
	RM	0.900	0.776	0.903	0.915	0.843
	SD	0.482	0.150	0.827	0.804	0.863
	SR	0.469	0.030	0.114	0.634	N/A
SAS	US	0.921	0.835	0.920	0.935	0.688
	RM	0.900	0.801	0.901	0.914	0.879
	SD	0.451	0.140	0.817	0.869	0.821
	SR	0.440	0.048	0.134	0.539	N/A

# Patterns of evolutionary constraint

## Methods

Patterns of evolutionary constraint across genes have been previously examined in SNVs and indels and quantified by the loss-of-function observed/expected upper bound fraction (LOEUF) score [7]. Analyses in gnomAD-SV V2 showed that SVs exhibit similar trends of gene-level intolerance to variation [2]. To demonstrate that the srWGS SV CDRv7 off-cycle callset exhibits the same fundamental biological signals, we replicated the methods in Collins et al. 2020 [2] to examine trends of SV constraint in comparison to SNV constraint. Briefly, we estimated the depletion of rare SVs per gene compared to the expected count of SVs per gene, using a negative binomial regression model.

We subsetted the VCF to sites with a PASS filter status, then to the maximal set of 94,181 unrelated samples in the CDRv7 off-cycle srWGS SV callset. Next, we computed the number of rare ( $AF < 1\%$ ) SVs observed per gene for all autosomal protein-coding genes, across four different classes of functional consequences. The functional consequence categories used in this analysis were predicted loss-of-function (pLOF), copy gain duplication (CG, in which an entire gene is duplicated), intragenic exonic duplication (IED, in which intact exons are duplicated without disrupting coding sequence), and spanning inversion (INV, in which an inversion spans an entire gene).

Based on gene characteristics and these observed counts, we trained a negative binomial regression model to predict the expected counts of SVs of different functional classes for each gene. We incorporated the following factors into the model: gene length, total and median exon length, total and median intron length, number of exons, number of introns, and the proportion of the gene overlapped by segmental duplication regions. We trained the model on the genes exhibiting relatively neutral selection in the 5th to 9th LOEUF deciles. We then applied the model to estimate the expected number of gene-disrupting SVs in each functional category across all autosomal protein-coding genes in GENCODE v39 [8].

We binned genes by LOEUF percentile (resulting in 100 bins containing an average of 189 genes each) and compared the estimated expected counts of rare SVs of each functional class for the genes in each bin to the observed counts. Finally, we used a two-sided Spearman's rank correlation test to assess the correspondence between SV and SNV constraint across all 100 bins of genes.

## Results

[Figure 5](#) shows the results of the constraint analysis for rare coding SVs across four different classes of SV functional consequences representing a spectrum of expected impact on the protein. As expected, the depletion of rare pLOF SVs shows the strongest concordance with the

depletion of pLOF SNVs as measured by LOEUF (pLOF Spearman correlation test,  $\rho=0.95$ ,  $P<10^{-100}$ ). There is also a strong relationship between CG SV constraint and LOEUF (CG Spearman correlation test,  $\rho=0.87$ ,  $P<10^{-100}$ ) and a weaker but significant relationship between IED SV constraint and LOEUF (IED Spearman correlation test,  $\rho=0.74$ ,  $P<10^{-100}$ ). There is not a significant correlation between INV constraint and LOEUF (INV Spearman correlation test,  $\rho=0.15$ ,  $P=1.47\times 10^{-1}$ ). These results recapitulate the findings in Collins et al. 2020 [2] and show that our findings reflect previously established patterns of evolutionary constraint.

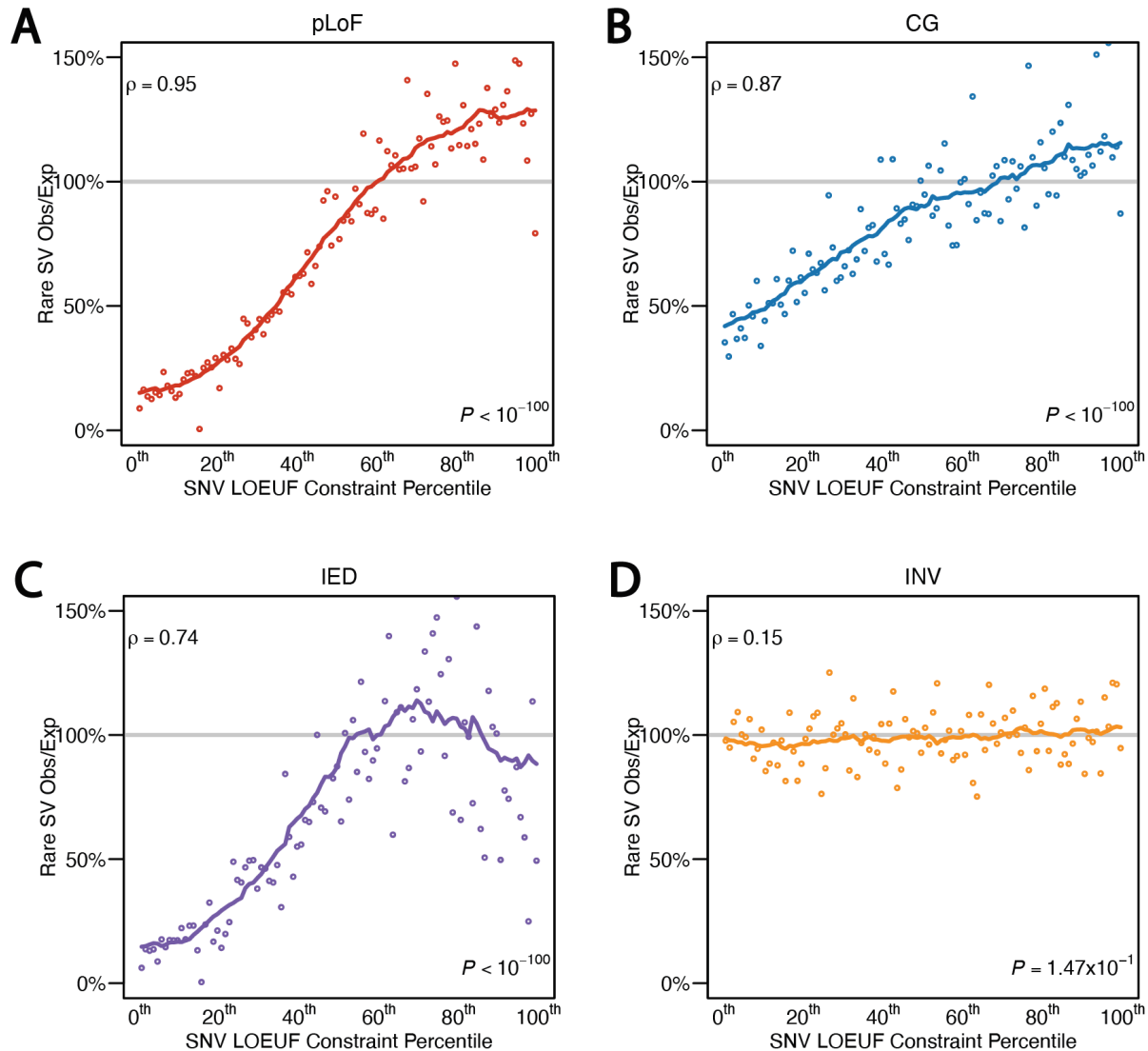


**Figure 5** – Comparing pLOF SNV constraint to binned SV constraint in four different SV functional classes: A) predicted loss-of-function (pLOF), B) copy gain duplications (CG), C) intragenic exonic duplications (IED), and D) inversions that span an entire gene (INV). Points represent binned observed vs. expected SV count ratios compared to the LOEUF percentile from SNVs. Solid lines represent 21-point rolling means. The results of the two-sided Spearman correlation test (the correlation  $\rho$  and the P-value) are superimposed on each panel.

# Comparisons to orthogonal data types

## Benchmarking against long-read PacBio sequencing

### Data and methods

We evaluated passing non-reference SV genotypes based on evidence derived from IrWGS. The IrWGS SV calls using existing algorithms can confirm SV events with accurate breakpoint resolution, but often miss large insertions and inversions near the IrWGS read size, as well as large copy number variants (CNV) that require read depth evidence to detect. Read depth signatures are used extensively in the GATK-SV short-read pipeline but not in existing IrWGS algorithms. Because of this reduced sensitivity of IrWGS SV calling to large SVs, variants larger than 5 kilobases (kb) were excluded from this analysis.

We performed this analysis on a subset of 97 samples with matched IrWGS data that were held out from training of the GQ filtering model used for refinement of the SV callset (see srWGS SV QC Report, Genotype Filtering [\[1\]](#)). For each sample, passing non-reference genotypes for eligible variants (SV type DEL, DUP, INS, or INV, with PASS filter status, below 5 kb in length) were assessed against IrWGS using the IrWGS validation tool VaPoR [\[9\]](#) and their overlap with SV calls from IrWGS data from the tools PAV [\[10\]](#), PBSV [\[11\]](#), and sniffles2 [\[12\]](#). Duplications present a challenge to overlap-based methods of variant matching, as they can be called either as INS or DUP types, with INS calls either at the 5' or 3' end of the duplicated sequence. In order to avoid such complications with variant representation, the evaluated calls were grouped into three main classes: insertions (encompassing insertions and duplications), deletions, and inversions prior to variant matching. srWGS variants were matched with IrWGS variants of the same comparison class by requiring 10% reciprocal overlap and 50% size similarity. This analysis was performed using the GATK SVConcordance tool [\[13\]](#).

### Results

The validation callset generated by GATK-SV included 768,579 total non-reference calls comprising 58,910 unique DEL, DUP, INS, and INV variants under 5kb. These calls were strongly supported by IrWGS, with 674,190 (88%) of the PASS genotypes confirmed by at least one IrWGS tool. [Figure 6](#) shows the distributions of support from IrWGS for insertion and deletion SVs, and [Figure 7](#) shows them for inversions. For each intersection, the number of calls is shown with variant size and GQ distributions. Note that the GQ recalibration model was trained on a set of independent samples using IrWGS support criteria. Therefore, a higher GQ reflects that the call was similar to calls in the training set with support from VaPoR and at least one of the three IrWGS SV algorithms (see srWGS SV Genotype Filter section of the Genomic Research Data Quality Report [\[1\]](#)).



There was a high degree of consensus among the IrWGS callers, with only 65,744 (9.8% of confirmed) srWGS SV calls supported by just one IrWGS SV caller and 565,608 (84%) supported by at least three. Calls with no IrWGS support had overall lower genotype quality (GQ) scores (median 47) compared to supported calls (median 89), which is consistent with expectations. Notably, PBSV was the most consistent with srWGS SV calls from GATK-SV, supporting 629,779 (93% of confirmed) srWGS calls with a median GQ of 89, compared to the remaining 44,411 IrWGS supported calls with a median GQ of 55.

The distribution of calls produced by the three non-depth based srWGS SV calling tools used by GATK-SV (Manta [14], Wham [15], and MELT [16]) and the fraction of calls with IrWGS support for each is shown in Figure 6B. Overall, Manta produced 622,921 (81%) of passing calls, 88% of which were supported by at least one IrWGS SV discovery method. In addition, MELT contributed 150,072 (20%) of the calls with 87% IrWGS support. Wham is utilized in this pipeline to access a subset of small duplications that are missed by other algorithms, with 99,718 variants retained after filtering (13% of total) and 87% IrWGS support. Similar to insertion and deletion SVs, inversions exhibited a high degree of support from IrWGS, with 859 of 889 (97%) validated (Figure 7).

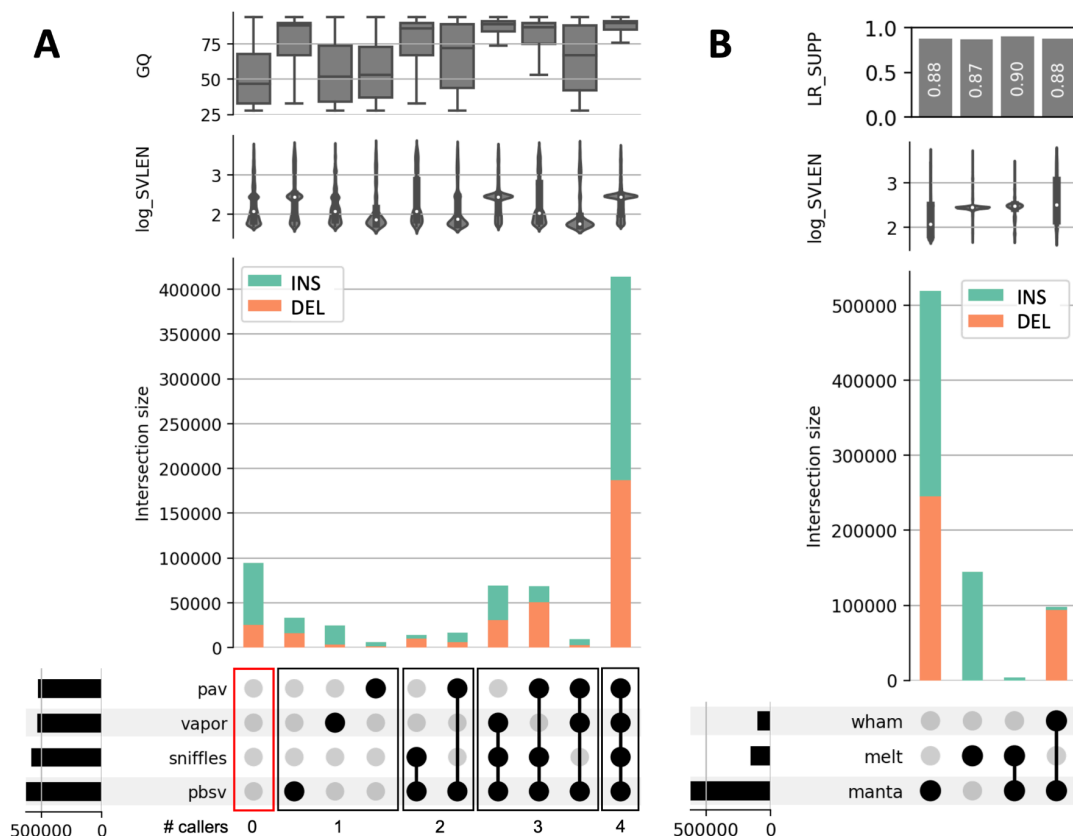


**Figure 6** – Evaluation of passing srWGS insertion and deletion calls under 5 kb against IrWGS tools. The insertion class encompasses all sequence gain events, including duplications. (A) Distribution of IrWGS tool support. Filled circles indicate combinations of tools that support the call counts in each column. Combinations with fewer than 5,000 total calls are omitted for clarity.

Violin plots of genotype quality and  $\log_{10}$  of variant length distributions are superposed over each combination. Total supported calls for each IrWGS tool are plotted at the bottom-left. (B) Distribution of srWGS tool support. Top panel shows the fraction of calls with support from at least 1 IrWGS tool. Combinations with fewer than 2,000 calls are omitted.

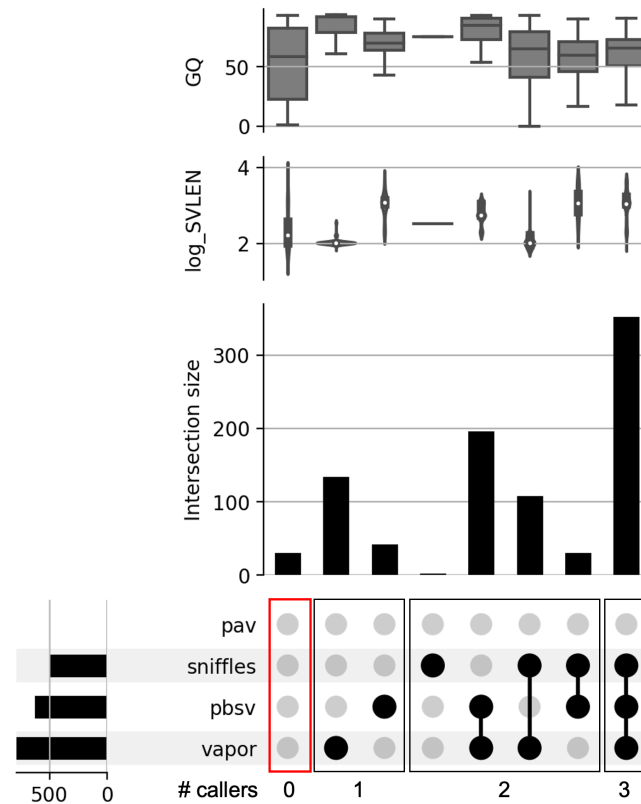


**Figure 7** – Evaluation of passing srWGS inversion calls under 5 kb against IrWGS tools. Data is plotted as in [Figure 6](#) for insertion and deletion calls but with all non-empty combinations shown.

## Benchmarking large CNVs against microarrays

### Data and Methods

In a randomly-selected subset of 10,000 samples, we evaluated all deletions and duplications greater than 10 kb and less than 10 Mb in length on the autosomes using array intensity data from the LRR field of the array VCFs (available on the Researcher Workbench and described in [‘How the All of Us Genomic Data are Organized’](#)). To conduct this evaluation we used the GenomeSTRiP IntensityRankSumAnnotator (IRS) tool [\[17,18\]](#). The IRS tool compares the array probe intensity values between samples predicted to carry the CNV and those predicted to be non-carriers (according to genotypes in the SV VCF), using all probes that are within the CNV interval. Using a non-parametric test, the IRS tool assigns a p-value to each CNV which

indicates if the CNV genotypes are supported by the intensity data. In addition to using site-level p-values, the authors of the test recommend [17,18] using IRS to calculate a callset level false discovery rate (FDR) by computing  $2 * \frac{M}{N}$ , where  $M$  is the number of sites where the IRS p-value is greater than 0.5 and  $N$  is the total number of sites. CNVs greater than 10 Mb were excluded due to the computational requirements required to evaluate array concordance using these methods and the fact that the majority of these large events are likely to be somatic events that can be challenging to confirm. We note that performance of this validation can be compromised for smaller CNVs if there is insufficient probe density in the CNV region on the microarrays, which is a common challenge for CNVs less than 20 kb in size. Nonetheless, this validation can still be informative in the 10-20 kb size range for many regions of the genome.

We ran the IRS test on all samples at each site. The IRS test requires that an intensity value be present for all samples. Therefore, if a sample had a missing data value for one or more of the probes covered by the CNV interval, we set the intensity value to a random value such that the rank of the inserted value within the cohort would be uniformly distributed. This was achieved by choosing another sample at random from the set of samples with non-missing values for that probe and setting the missing sample's intensity value to that of the randomly chosen sample. The substitution of missing data points with randomly chosen values was necessary for testing the callset against the entire cohort, but could inflate the FDR estimates provided by the IRS test.

## Results

After removing 1,654 CNV sites which did not overlap any array probes and could not be tested, 34,648 autosomal CNVs of size 10 kb to 10 Mb were evaluated using this test, including 20,347 deletions and 14,301 duplications. 215 out of 20,347 deletions had an IRS p-value greater than 0.5, resulting in an estimated FDR of 2.11% for all deletions tested using the callset-wide evaluation procedure described above. 93.5% of deletions were validated using a more stringent p-value cutoff of 0.01, which was the threshold used to select sites for molecular validation based on IRS results in a previous study [17]. The results for deletions in different size ranges are shown in [Table 2](#).

**Table 2 – Deletion SV array validation results, stratified by SV size**

Size range	Number of sites included	Estimated Callset FDR	P-value < 0.01
10-20kb	9,097	2.85%	8166 (89.8%)
20-50kb	5,414	1.74%	5,166 (95.4%)
50-100kb	2,673	1.57%	2121 (97.2%)
100kb-1Mb	3,008	0.87%	2,956 (98.3%)
1-10Mb	66	0%	66 (100%)

Out of the 14,301 duplications evaluated, 374 had a p-value over 0.5, resulting in an estimated callset FDR of 5.23%. 90.0% of duplications validated at the 0.01 p-value threshold. Duplication results by size range are shown in [Table 3](#). As in the discussion of array benchmarking for the CDRv7 release [\[4\]](#), we note that 6.9% (297 / 4,313) of duplications and 6.2% (530 / 8,567) of deletions between 10 kb and 20 kb span only one probe, reducing the statistical power of the IRS test to validate these events at the p-value < 0.01 level. Overall, these results show that large CNVs in this callset were strongly supported by microarrays, with a very low estimated FDR for both large deletions and large duplications.

**Table 3 – Duplication SV array validation results, stratified by SV size**

Size range	Number of sites included	Estimated Callset FDR	P-value < 0.01
10-20kb	4,313	6.77%	3,491 (80.9%)
20-50kb	3,948	4.91%	3,630 (91.9%)
50-100kb	2,319	4.31%	2,201 (94.9%)
100kb-1Mb	3,443	4.12%	3322 (96.5%)
1-10Mb	166	1.20%	164 (98.8%)

## References

- [1] “All of Us Research Program Genomic Research Data Quality Report, Structural Variant Supplemental Dataset release C2022Q4R9\_offcycle” *All of Us Research Program*, <https://support.researchallofus.org/hc/en-us/articles/27496716922900-All-of-Us-Short-Read-Structural-Variant-Quality-Report>
- [2] Collins, R.L., Brand, H., Karczewski, K.J. *et al.* A structural variation reference for medical and population genetics. *Nature* **581**, 444-451 (2020). <https://doi.org/10.1038/s41586-020-2287-8>
- [3] Byrska-Bishop, Marta *et al.* “High-coverage whole-genome sequencing of the expanded 1000 Genomes Project cohort including 602 trios.” *Cell* vol. 185,18 (2022): 3426-3440.e19. doi:10.1016/j.cell.2022.08.004
- [4] “Benchmarking and quality analyses on the All of Us v7 short read structural variant calls”, *All of Us Research Program*, <https://support.researchallofus.org/hc/en-us/articles/14941865780500-Benchmarking-and-quality-analyses-on-the-All-of-Us-short-read-structural-variant-calls-ARCHIVED>
- [5] Hill, W G, and A Robertson. “Linkage disequilibrium in finite populations.” *TAG. Theoretical and applied genetics. Theoretische und angewandte Genetik* vol. 38,6 (1968): 226-31. doi:10.1007/BF01245622

- [6] Zhao, Xuefang et al. "Expectations and blind spots for structural variation detection from long-read assemblies and short-read genome sequencing technologies." *American journal of human genetics* vol. 108,5 (2021): 919-928. doi:10.1016/j.ajhg.2021.03.014
- [7] Karczewski, K.J., Francioli, L.C., Tiao, G. *et al.* **The mutational constraint spectrum quantified from variation in 141,456 humans.** *Nature* 581, 434–443 (2020).  
<https://doi.org/10.1038/s41586-020-2308-7>
- [8] Frankish A, Diekhans M, *et al.* GENCODE reference annotation for the human and mouse genomes. *Nucleic Acids Res.* 2019 Jan 8;47(D1):D766-D773. doi: 10.1093/nar/gky955. PMID: 30357393; PMCID: PMC6323946.
- [9] Zhao X, Weber AM, Mills RE. A recurrence-based approach for validating structural variation using long-read sequencing technology. *Gigascience.* 2017 Aug 1;6(8):1-9. doi: 10.1093/gigascience/gix061. PMID: 28873962; PMCID: PMC5737365.
- [10] P. Ebert, P. A. Audano, Q. Zhu et al., Haplotype-resolved diverse human genomes and integrated analysis of structural variation. *Science* **372**, eabf7117 (2021).
- [11] [10] **PacBio structural variant calling and analysis tools (PBSV)**, Retrieved March 3, 2023, from <https://github.com/PacificBiosciences/pbsv>.
- [12] Sedlazeck FJ, Rescheneder P, Smolka M, et al. Accurate detection of complex structural variations using single-molecule sequencing. *Nat Methods.* 2018 Jun;15(6):461-468. doi: 10.1038/s41592-018-0001-7. Epub 2018 Apr 30. PMID: 29713083; PMCID: PMC5990442.
- [13] GATK Team "SVConcordance (Beta) – GATK." *GATK*, 20 Mar. 2023, <https://gatk.broadinstitute.org/hc/en-us/articles/13832773767963-SVConcordance-BETA->.
- [14] Chen, X. *et al.* (2016) Manta: rapid detection of structural variants and indels for germline and cancer sequencing applications. *Bioinformatics*, 32, 1220-1222.  
[doi:10.1093/bioinformatics/btv710](https://doi.org/10.1093/bioinformatics/btv710)
- [15] Kronenberg ZN, Osborne EJ, Cone KR, Kennedy BJ, Domyan ET, Shapiro MD, *et al.* (2015) Wham: Identifying Structural Variants of Biological Consequence. *PLoS Comput Biol* 11(12): e1004572. <https://doi.org/10.1371/journal.pcbi.1004572>
- [16] Gardner, E. J., Lam, V. K., Harris, D. N., Chuang, N. T., Scott, E. C., Mills, R. E., Pittard, W. S., 1000 Genomes Project Consortium & Devine, S. E. The Mobile Element Locator Tool (MELT): Population-scale mobile element discovery and biology. *Genome Research*, 2017. **27**(11): p. 1916-1929.
- [17] Mills, Ryan E et al. Mapping copy number variation by population-scale genome sequencing. *Nature* vol. 470,7332 (2011): 59-65. [doi:10.1038/nature09708](https://doi.org/10.1038/nature09708)
- [18] Handsaker, R., Van Doren, V., Berman, J. *et al.* Large multiallelic copy number variations in humans. *Nat Genet* **47**, 296-303 (2015). <https://doi.org/10.1038/ng.3200>